Journal of Electroceramics 3:3, 245–254, 1999

4-Probe Micropatterning and Electrical Measurements Across Individual Grain Boundaries in Electroceramics

RICHARD P. RODRIGUES, JIN-HA HWANG & VINAYAK P. DRAVID
Department of Materials Science and Engineering, Northwestern University, Evanston, IL 60208

Submitted September 1, 1998; Revised November 19, 1998; Accepted December 14, 1998

Abstract. A novel approach combining conventional contact- and projection-lithography techniques has been devised to implement microelectrodes, down to submicron size, across isolated site-specific features as small as 2–3 micron. For both *ex-situ* and *in-situ* electrical characterization, such features of interest are isolated interfaces and grain boundaries in electroceramics and multilayer devices, including those in as-prepared TEM specimen. The procedure has been discussed for implementing 4-probe microelectrodes across several individual isolated grain boundaries of a commercial ZnO varistor containing 2–10 micron size grains. In addition, we discuss the results from dc 4-probe I-V and ac 2-probe impedance measurements across individual grain boundaries, and dc 2-probe I-V and ac 2-probe impedance measurements from grain interiors isolating these grain boundaries. Over and above the generally observed properties of isolated grain boundaries, the measurements reveal (1) inhomogeneity and applied-bias-polarity dependent asymmetry in the nonlinear I-V characteristics of grain boundaries, (2) possible presence of non-ohmic electrode-ceramic contact resistance in 2-probe measurements, and (3) a gradual process of irreversible degradation of the nonlinear I-V behavior with respect to thermal runaways upon application of a dc bias across isolated grain boundaries.

Keywords: contact lithography, projection lithography, microelectrode patterning, varistor, zinc oxide, grain boundaries, I-V measurements, ac impedance spectroscopy, Schottky barrier, nonlinearity, breakdown voltage, asymmetric behavior, degradation

1. Introduction

Nonlinear electrical properties of electroceramics such as varistor, thermistor and barrier layer capacitor (BLC) are directly linked to the electrically active interfaces and grain boundaries (GBs) [1,2]. The nonlinear electrical activity is generated upon formation of the electrical barriers across the GBs due to segregation or second-phase formation of the additives at and near the GB region. The electrical barriers make the GBs highly resistive compared to the grain interiors and the breakdown of these barriers under higher applied electrical or thermal fields gives rise to the nonlinear properties. Since the overall nonlinear character of a bulk electroceramic is a cumulative effect caused by individual GBs, the importance of understanding the I-V character and the microstructure of the individual GBs has long been recognized [3–14].

Polycrystalline zinc oxide is such an electroceramic exhibiting excellent varistor behavior. The nonlinearity is identified by high (> 30) values of the exponent α, which is defined such that it empirically describes the nonlinear I-V behavior as $I \propto V^{\alpha}$. High values of α are achieved by incorporating oxide additives, mainly of Bi and other metals like Mn, Co, Ni, and Sb. These additives segregate or form second-phases at and near the GB region creating electrical barriers across the GBs. A number of researchers have performed I-V measurements probing the nonlinear character [3–13] and analytical studies probing the chemical nature of individual GBs [11,12,14]. For I-V measurements, either external direct-contact probes were used across individual GBs [3–5] or electrodes

were implemented across individual GBs by metal evaporation through photolithography [6–9,11,12]. Further investigations have also been carried out across individual GBs using techniques such as SEM voltage-contrast [9], SEM electron-beam-induced-current (EBIC) [9,10], analytical electron microscopy (AEM) [11] and deep level transient spectroscopy (DLTS) [12] to complement the I-V measurements. The investigations by Olsson and Dunlop are particularly informative [11]. They measured the I-V behavior of individual GBs of ZnO specimens prepared for TEM and subsequently performed AEM to identify four types of GBs: (1) GBs with thin Bi-Rich $\sim 2\,\text{nm}$ intergranular film, (2) GBs without secondary phases, but with Bi segregation, (3) GBs with thick intergranular region of Bi_2O_3 and grains of spinel, and (4) GBs with thick layer of pyrochlore and grains of spinel. They observed higher breakdown voltage for GBs with intergranular film due to introduction of additional interface states.

All of these measurements [3–13] were performed across individual GBs using 2-probe technique. They do not address any contact resistance involved with interfaces between dissimilar materials while investigating interfaces between similar materials. As identified below, 2-probe measurements could suffer from non-ohmic contact resistance between the ceramic and the external metal electrodes. We are aware of only one report on 4-probe measurements, which were performed across individual GBs in ZnO ceramics using direct-contact probes [13]. All of the above measurements required ceramics of large grain size (25–150 μm) to establish external contacts. In addition, I-V and ac impedance measurements on the grain interiors separating the GBs have been ignored in the 2-probe technique. In order to perform such *ex situ* measurements, it is necessary to design a procedure availing implementation of 4-probes across individual GBs.

There is also a growing need to understand the nanoscale role of GBs and additives in connection with the nonlinear properties of electroceramics. In this regard, it is important to investigate across individual GBs, the functional dependence of the nanoscale variations in (1) the chemical and electronic structures and (2) the GB double Schottky barriers, on the applied electrical or thermal fields. Such dynamic functional dependence can be understood only by utilization of diverse TEM analytical techniques under dynamic *in situ* conditions. Such investigations however, have remained elusive due to experimental difficulties. One of these difficulties is the inability of implementing electrodes across individual GBs on an electron transparent TEM specimen for isolating the GBs for *in situ* dynamic investigations. Thus, it is necessary to design a procedure availing implementation of 4-probes across individual GBs, also for *in situ* measurements.

Towards these ends, we establish in this paper an approach combining contact- and projection-lithography techniques to conveniently implement microelectrodes across isolated site-specific features for both *ex situ* and *in situ* investigations. The procedure allows implementation of 4-probe electrodes across isolated GBs or on isolated grain interiors for grain sizes as small as 2–3 μm with probe separations as small as 0.5 μm. It has been used for successful implementation of 4-probe electrodes across individual GBs of both bulk and *TEM specimen* of ZnO varistors. It is, therefore, possible to conduct both *ex situ* and *in situ* investigations not performed before. In this paper, we discuss the lithography procedure for both bulk and TEM specimen and the results only from the investigations for bulk specimen of a commercial ZnO varistor. In particular, I-V and ac impedance measurements were performed across individual GBs and on the grain interiors from either side of the GBs. *In situ* TEM investigation are underway and the results will be discussed in future.

2. Specimen and Photolithography

Commercial ZnO varistors identified as V130LA10 310 GE with grains 2–10 μm in size were used in this study. A lift-off technique was used to implement several sets of 4-probe microelectrodes on polished surfaces of these varistors. Care was taken to minimize surface grain pull-out during polishing in order to insure the spinning of resist with uniform thickness over the entire surface and the continuity of the metal electrodes without any breaks. The polished surfaces were slightly etched in 10% concentrated HNO_3 for 3 s to locate the grain boundaries clearly. Two different masks were designed; one each for contact lithography and projection lithography. Several sets of 4-probe patterns were developed on the resist-covered surfaces through contact lithography. Following metal deposition and metal lift-off discussed below, this patterning creates sets of 4-

probe square electrodes on the surfaces of the varistors as shown in Fig. 1(a). The individual electrode is 0.475 square mm in size enabling easy external connections using 70 micron silver wires. Prior to metal deposition, the patterns of 4-probe square developed by contact lithography were extended further across individual grain boundaries. The extensions were patterned by aligning in projection lithography a second mask across an individual grain boundary located in the central region of Fig. 1(a). The central regions were exposed with the mask projected at 100 × for all sets of 4-probe squares and then developed. Since it is possible to locate the GBs underneath the resist with visible light, the projection mask can be aligned across a specific GB in the central region. Following metal deposition and metal lift-off discussed below, this patterning creates microelectrodes as shown in Fig. 1(b). Thus, unlike all previous methods, the combination lithography procedure is site specific and has a distinct advantage that it implements microelectrodes across single isolated GBs for all the patterns laid on the substrate. The site specificity makes it even easier to implement 4-probe patterns on isolated grains with this procedure. The procedure can also be used to isolate specific single interfaces in thick multilayer devices for electrical characterization.

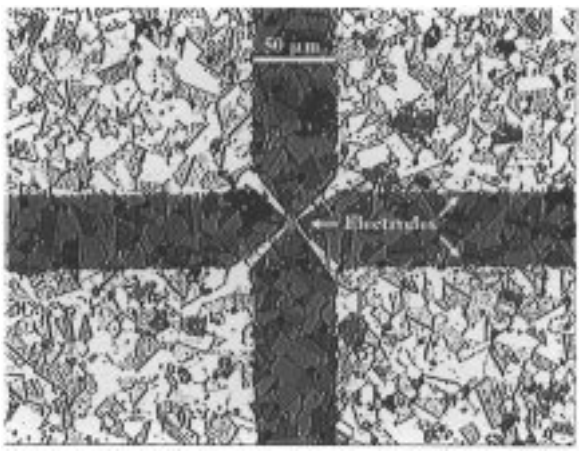

(a)

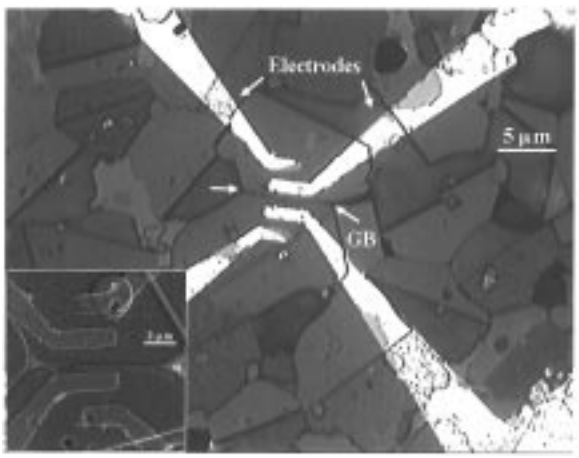

(b)

Fig. 1. (a) A pattern of 4-probe square-electrodes implemented on ZnO varistor surface. (b) Microelectrodes extended across individual grain boundaries of ZnO in the central region of (a). Inset shows SEM micrograph for a different GB.

The masks were redesigned to implement 4-probe electrodes across isolated GBs of the TEM specimen. Due to small size of the TEM specimen (3 mm), both the masks were used in projection, one at 5 × to develop sets of outer 4-probe electrodes and the other at 40 × to extend each of the sets across specific single GBs. In all, 24 outer electrodes were designed on the TEM specimen and extended across 8 isolated GBs. Figure 2 shows optical micrographs of the patterned TEM specimen before ion-beam-thinning treatments. The 4-probe extensions patterned at 40 × can be seen to isolate single GBs. Following the sequence of contact exposure and developing, and projection exposure and developing for the bulk and TEM specimens, metal electrodes were implemented on the patterned resist. The electrodes consisted of a bottom layer of Ni for good adhesion with the electroceramic and a top layer of Ag, both of thickness ~ 50 nm. These layers were sequentially evaporated over the entire surface and patterned metal electrodes were created upon removing the unwanted metal through the lift-off process, i.e., by etching the resist underneath the metal layers. The investigation of the TEM specimen is underway; that of the bulk specimen is discussed below.

3. Electrical Measurements

I-V measurements were performed using a Keithly 220 programmable dc current source and a Keithly 196 System DMM digital multimeter. To eliminate electrode-ceramic contact resistance, current in the range 10^{-8} A–10^{-1} A was applied using the outer set of electrodes and the inner set was used to measure the

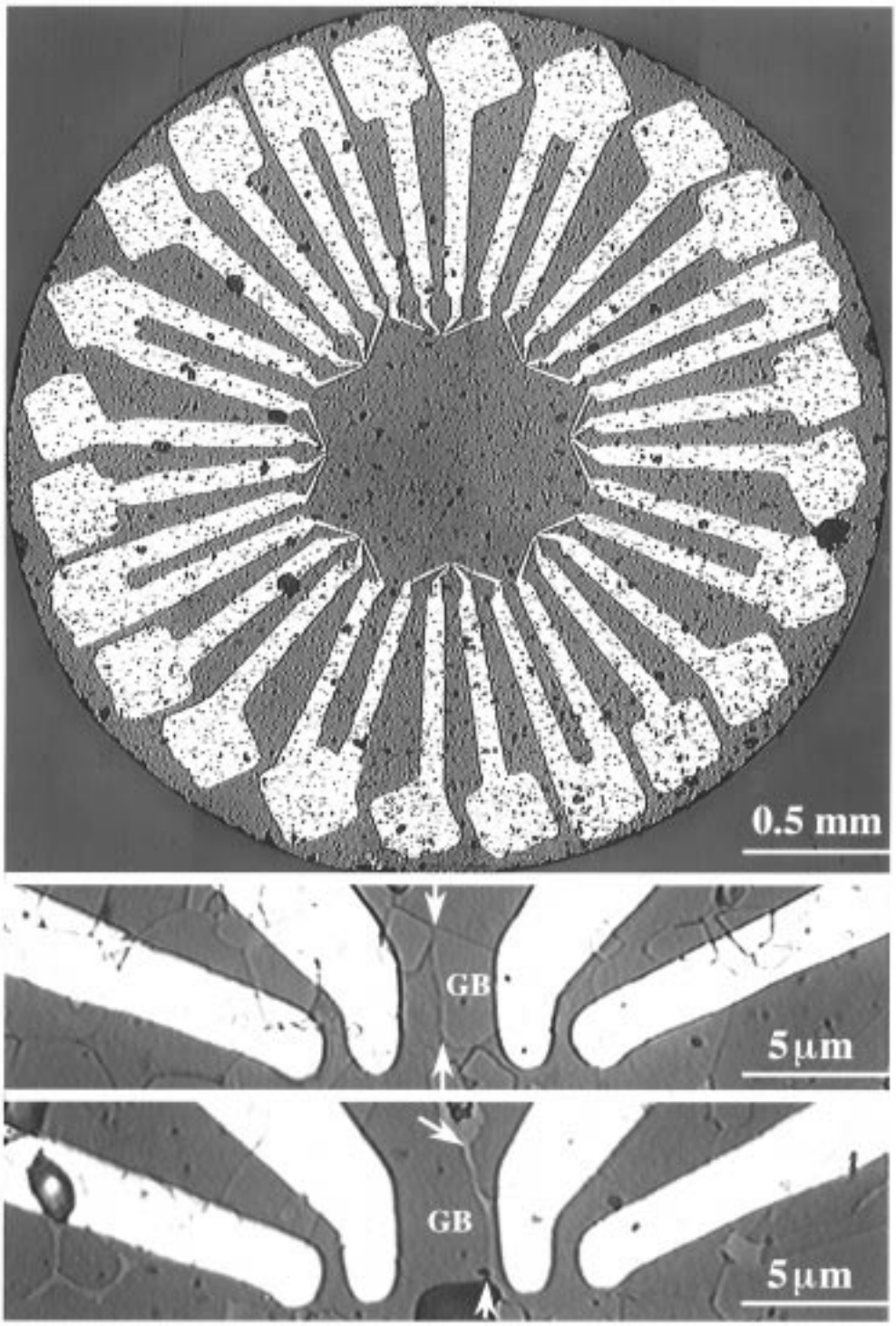

Fig. 2. A pattern of 4-probe electrodes implemented on a ZnO TEM specimen. The extensions isolating two single grain boundaries are shown.

voltage across the GBs. The polarity was switched at every value of applied current to alternately forward and reverse bias the GBs. Since, the 4-probes were not implemented on single grains, only 2-probe I-V measurements were performed on the grain interiors separating the GBs. Additionally, ac 2-probe impedance measurements were performed on the GBs and on the grain interiors separating the GBs in the frequency range 5 Hz–13 MHz using an HP-4192A low-frequency impedance analyzer.

Metal electrodes extended up to the grains across both sides of the individual GBs are actually laid on a large region of the ceramic in this and other investigations [6–9,11,12]. Therefore, the isolated GB of interest experiences an effective parallel network associated with many other GBs present underneath and between different sections of the electrodes. Such network is present even when measurements involve employment of external direct-contacts with the ceramic [3–5]. The conductive grains are separated by the highly resistive GBs that are interconnected in the three dimensions by a skeleton of resistive second phases surrounding the grains. Therefore, the effective parallel network experienced by the GB of interest is composed of highly resistive percolative paths along the GBs. The network is also composed of highly resistive grain-to-grain conduction paths across a series of GBs between the electrodes. Outward from the microelectrodes, towards the large outer electrodes, the spreading resistance of the electrodes should decrease due to increasing area of contact if the material underneath is uniformly resistive [15]. However, due to the increasing complexity of the network of percolative paths and grain-to-grain paths within and outside the region of the spreading resistance ($\sim$ twice the region of electrode contacts [15]), the spreading resistance, as well as, the total resistance between the electrodes increases by several orders of magnitude. Therefore, very small amounts of percolative and grain-to-grain currents will flow between the outer region of the electrodes. Since such small currents are incapable of producing GB breakdown fields, the outer GBs can be considered almost open ended.

The spreading resistance of the microelectrodes closer to the GB of interest should increase (due to decreasing contact area) if the material underneath is uniformly resistive. Dramatic increase in the spreading resistance of the outer large electrodes is inevitable in presence of the GBs. However, no GBs are present within the region of the spreading resistance ($2\,\mu$m) of the microelectrodes as this region is smaller than the average grain size ($> 4\,\mu$m). Therefore, the microelectrodes still provide the best conduction path for substantial applied current to appear across the GB of interest.[1]

Nonetheless, apart from flowing directly across the GB and along percolative paths, this current can also flow across other GBs in the vicinity of the GB of interest. If such parallel currents are large enough to produce breakdown fields, the nonlinear behavior of GBs in those paths should also be observed (as additional breakdown(s) in the prebreakdown and/or upturn regions). Therefore, in a given I-V measurement across an individual GB, there exists a possibility of detecting multiple nonlinear behaviors at different voltages and in different ranges of applied currents. Here, different voltages correspond to the collective breakdowns of all the GBs across individual parallel paths. These breakdowns are initiated in different ranges of applied currents that enable sufficient breakdown-causing currents to flow across such parallel paths. Any interfaces such as metal-ceramic contact, which is in series with the GB of interest, do not show separate breakdowns, but, as in the measurements across a bulk specimen (containing a series of GBs), simply elevate the I-V characteristic to higher voltages and currents.

Since percolative paths are present irrespective of the nature of the breakdown (single-GB or multiple-GBs), as per the discussion above, the actual current causing the breakdown differs somewhat from the applied current in this and the other investigations [3–13]. This situation makes it difficult to accurately estimate the current density at which nonlinearity is observed across an individual GB. In this respect and also in view of presence of any contact (ohmic and non-ohmic) resistance, the measurements should be interpreted with caution. The issue could, however, be addressed independently by investigating 4-probe I-V characteristics of model designs containing single varistor hetrojunctions [16,17].

4. Results

Figure 3 shows two sets of I-V measurements for two different GBs. In the first set, nonlinear behavior is observed across both GBs for both polarities of applied current with Schottky barrier breakdown

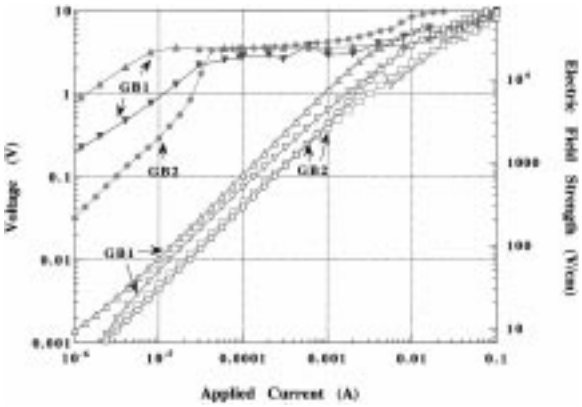

Fig. 3. Two sets of dc 4-probe I-V measurements across two isolated grain boundaries of ZnO. The bottom set corresponds to post-permanent-breakdown measurements.

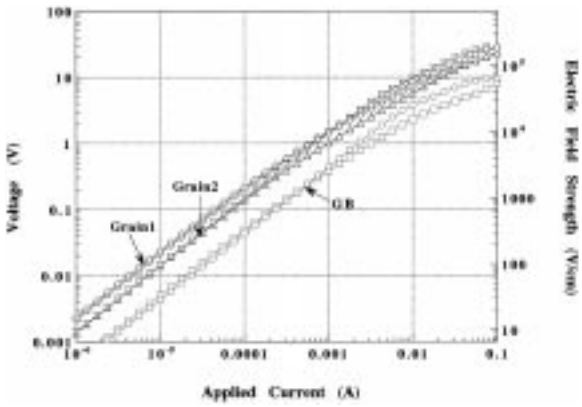

Fig. 4. dc 4-probe post-permanent-breakdown I-V measurements across one of the grain boundaries of Fig. 3 and dc 2-probe I-V measurements from the grain interiors isolating this grain boundary.

occurring at ~ 2.5 V. The nonlinear behavior is observed to be symmetric with respect to the polarity of the applied current. Such GBs have been identified as GBs without secondary phases, but with Bi segregation [11]. In the prebreakdown ohmic region, the I-V behavior under forward bias differs somewhat from that under reverse bias. This difference stems from the variations in the percolative current paths provided by the network of GBs and the skeleton of second phases for the two biases [11]. Subsequent forward and reverse biased measurements as shown by the second set of I-V plots in Fig. 3 did not reproduce the nonlinear character for both the GBs. The likely cause is that the GBs suffered permanent degradation and underwent an irreversible loss of nonlinearity.

In addition to dc 4-probe I-V measurements, ac 2-probe impedance measurements were performed across individual GBs. dc 2-probe I-V and ac 2-probe impedance measurements were also performed on grains on either side of the GBs. Figure 4 shows (1) the dc 4-probe I-V behavior of one of the GBs from Fig. 3 after permanent degradation and (2) dc 2-probe I-V behavior of grain interiors on either side of this GB. The GB can be expected to show I-V behavior similar to that of the grains after permanent loss of nonlinearity. It can be seen from Fig. 4 that the resistances of grain interiors are higher than that of the degraded GB and somewhat nonlinear. Also, the resistances of grain interiors differ from each other. The increase and the difference in grain resistances could be arising from different grain orientations and/or be due to the non-ohmic and ohmic metal-ceramic contact resistances associated with the dc 2-probe I-V measurements of the grain interiors. Any non-ohmic contributions should presumably be discernible as separate well-defined semicircles in the impedance spectra. The 2-probe impedance plots measured from the set of electrodes containing the GB in Fig. 4 are shown in Figs 5(a) and 5(b) for ac frequencies ranging from 5 Hz to 13 MHz. Once again, the resistances of the grain interiors taken at 5 Hz ($\sim$ dc) differ, but are close to the slopes obtained from the I-V behavior of these grain interiors in Fig. 4. In Fig. 5(a), there is a hint of separate semicircles for one of the grains, suggesting presence of non-ohmic contact resistance. Otherwise, the resistances measured for the grains contain the ohmic contact resistances and the intrinsic grain resistances. Just as for the grains, the 2-probe resistance of the GB taken at 5 Hz ($\sim$ dc) from Fig. 5(b) is close to that obtained from its pre-breakdown slope in Fig. 3. After comparing the dc resistances, it is quite clear from Figs. 4 and 5 that the resistivity of the undegraded GB is orders of magnitude higher than that of the grain interiors and any non-ohmic/ohmic contacts. Impedance measurements were performed for several sets of 4-probe patterns and similar results were obtained for the GBs and the grain interiors. The possibility of incorporating non-ohmic contact resistances in the measurements of the grain interiors can be eliminated by performing 4-probe measurements on each of the two grains across the GB.

In order to illustrate the dependence of GB permanent degradation on high applied fields, current

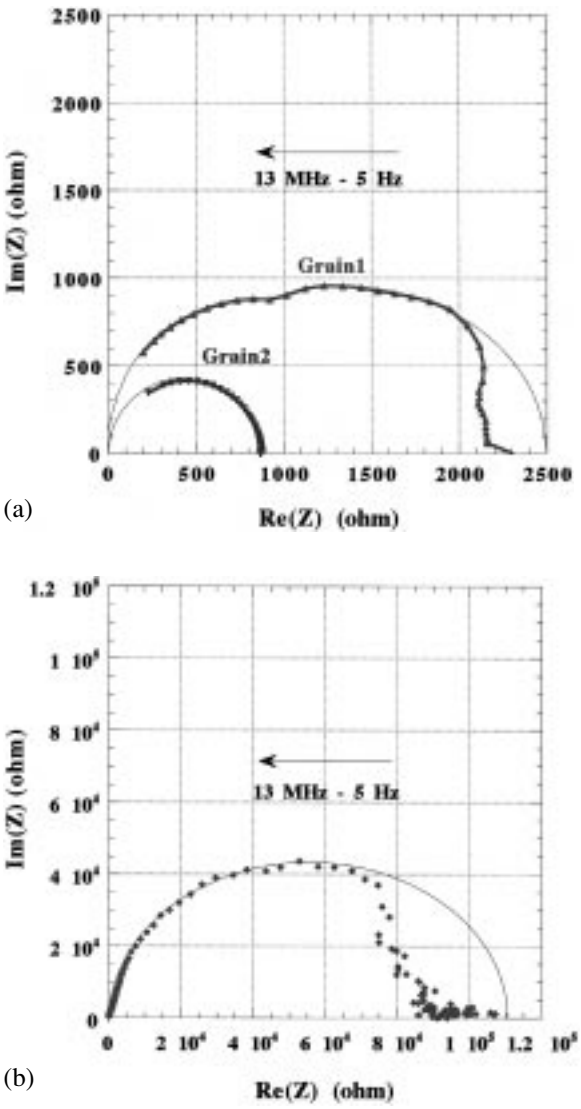

Fig. 5. ac 2-probe impedance measurements from (a) the grain interiors isolating the grain boundary and (b) the grain boundary of Fig. 4.

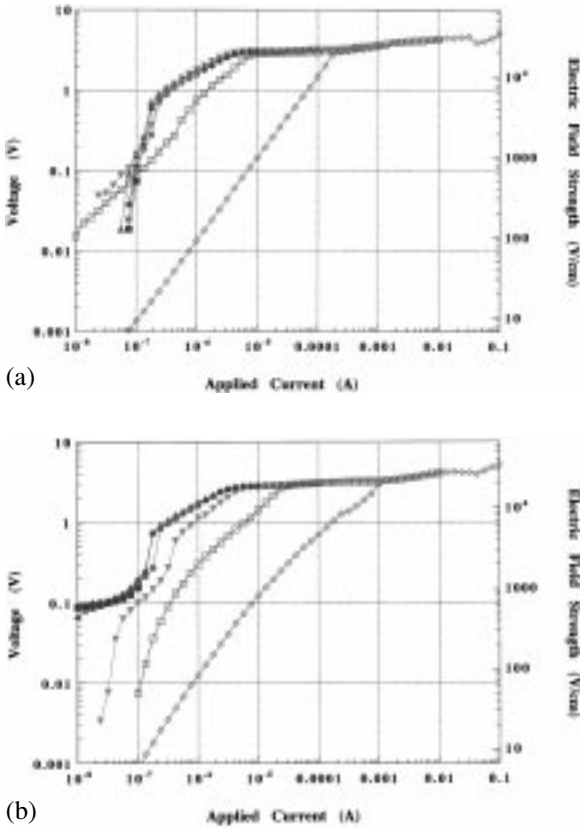

Fig. 6. dc 4-probe I-V measurements in (full)back-and-(incremental)forth steps for (a) forward and (b) reverse polarities of applied current across an isolated grain boundary of ZnO.

was applied in (full)back-and-(incremental)forth steps for measurements across remaining individual GBs. Figures 6(a) and 6(b), and 7(a) and 7(b) show these measurements for two different GBs for both polarities of the applied current. It can be seen that as the applied current is increased the nonlinear region gradually becomes narrow in the current range until the nonlinearity is partially or completely lost at higher current. Thus, the permanent degradation is a gradual and cumulative process once the barrier breakdown is achieved. The phenomena of degradation of bulk varistor has been investigated extensively and the behavior observed in Figs. 6 and 7 is similar to the degradation behavior observed for bulk I-V measurements performed at different temperatures [18–23], under prolonged ac or dc bias [23–26] or under high impulse-currents [27–31]. Since the nonlinearity is not reversible, thermal runaways must be the cause of permanent degradation. Joule heating effects caused by high current across isolated GBs are responsible for such thermal runaways. A considerable fraction of the heat generated across the GB will conduct more rapidly along the implanted metal electrodes. If the heat generated by the applied current across the GB is capable of reaching the melting and/or evaporation temperatures of GB additives, damage to the microelectrodes and to the grains and GBs underneath can be expected in the vicinity of the GB under investigation. Indeed, such minor post measurement damages were discernible in most cases and in a

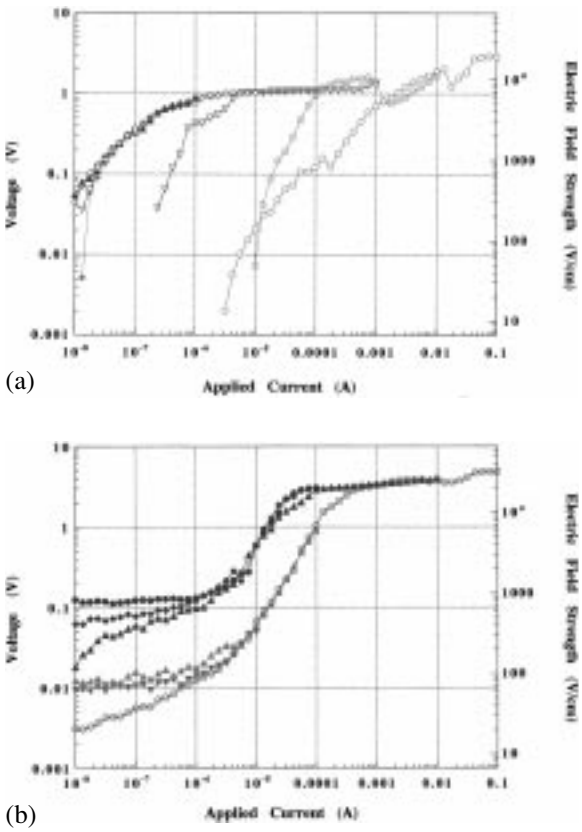

Fig. 7. dc 4-probe I-V measurements in (full)back-and-(incremental)forth steps for (a) forward and (b) reverse polarities of applied current across an isolated grain boundary of ZnO.

few cases the microelectrodes and the grains underneath suffered severe damages, along with physical degradation of the GBs under investigation.

The issue of electrical degradation of individual GBs has been investigated by several authors by performing I-V measurements across individual GBs, with an overloading current pulse [4], at higher temperature [6,9,17], under electrical aging of the varistor [32] or at room temperature after constant dc bias treatment at elevated temperature [11]. Degradation in nonlinear behavior was observed as a decrease in the range of the nonlinear region of the individual GBs [6,9,12,17,32]. The I-V behavior of single GBs were also rendered that of a single junction diode after degradation [4]. Various degradation mechanisms have been discussed by several authors [19,33,34]. These mechanisms include ion migration related to the interstitial Zn ions in the depletion region as main cause of degradation [33,35,36] and degradation caused by evaporation of Bi_2O_3 segregation layer at elevated sintering and/or measurement temperatures [18,23]. The degradation has also been associated with the reduction in oxygen [37], trapping of electrons [38] or asymmetry in the distribution of additive metal ions [14] at the GBs. Whatever the cause, the degradation of I-V behavior is a manifestation of the change in the Schottky-barrier height [19].

As shown in Fig. 7, the nonlinear behavior was observed to be asymmetric with respect to the polarity of the applied field for many GBs. For the GB of Fig. 7, breakdown voltage of 1 V is obtained for forward polarity and between 2-3 V for reverse polarity. Such observations of polarity dependent asymmetry in the nonlinear region of individual GBs have been made previously in the 2-probe measurements at higher temperatures [6] and during single GB degradation studies of the varistor [32]. Schwing and Hoffmann suggested that if the Schottky-type depletion layers are caused by electronic states, polarity-dependent asymmetry should be observed in the I-V characteristics [17]. Indeed, in their study of macroscopic model of microcontacts using single-crystals ZnO plates with a layer of oxide additives, they observed the ZnO/Bi_2O_3 junctions to be asymmetric in its I-V characteristic. Breakdown voltage of 3.2 V was obtained for one polarity and 2.4 V for reverse polarity [17]. In their 2-probe measurements, Olsson and Dunlop observed polarity dependent asymmetric I-V characteristic only across the ZnO/Bi_2O_3 junctions [11]. The asymmetry is associated with the difference between the band gap energy of ZnO and Bi_2O_3 and also with the differences in the position of the conduction band with respect to the Fermi level as experienced by the electron transport under different polarities.

One of the puzzling aspects of I-V characteristics which has not been seen before, is the observation in this study of two distinct breakdown regions as seen in Figs. 6(b) and 7(b). The higher voltage breakdown is identified as the breakdown of the GB under investigation. As per the discussion in section 3, the lower voltage breakdown appearing at 0.1 V corresponds to a breakdown of an interface parallel to the GB under investigation. However, since this breakdown voltage is very small it can not be associated with any of the GB types identified by Olsson and Dunlop [11]. It is not connected with a breakdown of any possible non-ohmic electrode-ceramic contact resistance since only 4-probe measurements were performed across the GB. Even if such a resistance

was involved in the measurements, it would be in series with the GB under investigation and would only elevate the GB I-V behavior to higher voltages and currents rather than creating a separate breakdown region. On one hand, the breakdown appearing at 0.1 V can be simply ignored as an artifact related to the instrument noise at smaller applied currents. Interestingly, however, it was observed only for some of the GBs, especially GBs showing asymmetric nonlinearity. Therefore, on the other hand, it is plausible to associate the breakdown to a parallel path for conduction of a very small current along the GBs that form the outer edges of the two grains separating the GB under investigation. These GBs along the edges must be such that they do not contain any resistive phases. The parallel path would then encounter a small nonlinear barrier formed by the second phase at the triple junction of the grain edges and the GB of interest. It is interesting to note that this breakdown degrades to ~ 0.01 V. If it indeed is a parallel path as suggested, the degradation is probably due to the evaporation of the second phase from the GB and from the triple junction (see Note).

I-V characteristics of about twenty GBs were investigated and four GBs did not show any significant nonlinearity. Such ohmic GBs have been encountered in some of the previous measurements [5,11,12] and identified to be containing pyrochlore and grains of spinel as no distinct varistor behavior between $ZnO/Zn_2Sb_3Bi_3O_{14}$ (pyrochlore) interface was observed [11]. The voltage corresponding to an onset of a breakdown varied in the range of 1-4 V in present investigation. The asymmetric GBs exhibited polarity dependence both for breakdown voltage and breakdown onset current.

5. Conclusions

In this paper we have presented an approach combining contact- and projection-lithography techniques for implementing 4-probe electrodes across individual interfaces in electroceramics. The procedure has been used for the first time to implement 4-probe microcontacts across single grain boundaries of a ZnO varistor material and extended to TEM specimen. It can be easily used to implement 4-probe microcontacts on isolated grain interiors and across specific single interfaces in multilayer devices. The distinct advantage of this technique is that site-specific features can be isolated for electrical characterization from features as small as 2–3 μm. We, therefore, expect the approach to be very useful in other interfacial systems containing submicron features.

Apart from previously reported observations, such as, (1) variation in the breakdown voltage from boundary to boundary, (2) asymmetry in the nonlinear I-V character of some of the grain boundaries with respect to the polarity of the applied bias and (3) ohmic nature of some grain boundaries, new interesting features of ZnO varistors have been incorporated in this paper. These include (1) the ability to perform I-V and impedance measurements across individual grain boundaries and on isolated grain interiors, (2) the observation of a possible double breakdown for some of the asymmetric grain boundaries and (3) the deduction that the 2-probe measurements could be complicated by the non-ohmic electrode-ceramic contact resistance. The I-V and ac impedance characteristics reveal the grain boundaries to be orders of magnitude more resistive than the grain interiors. Also interesting is the observation of a gradual process of degradation (irreversible loss of nonlinear I-V behavior) upon application of a dc current across isolated grain boundaries.

Acknowledgments

Research supported by the Basic Energy Science Division of U. S. DOE, under Grant Nos.: DE-FG02-92ER45475. The authors would like to thank Prof. Ketterson of Department of Physics, Northwestern University for access to his clean-room facility.

Note

1. Proof of this are the facts that (1) the observed breakdown voltage corresponds to that of a single GB (this GB must be the GB of interest as it offers the least resistive grain-to-grain conduction path between the electrodes), and (2) the microelectrodes suffer damage near the GB of interest after permanent degradation of nonlinear behavior of this GB.

References

1. L.M. Levinson (editor) in *Grain Boundary Phenomena in Electroceramics, Advances in Ceramics*, Vol. 1, (Am. Ceram. Soc., Columbus, OH, 1981).

See an excellent reference by D.R. Clarke, *J. Am. Ceram. Soc.,* **82** (3), 485 (1999).
2. M.F. Yan and A.H. Heuer (editors) in *Character of Grain Boundaries, Advances in Ceramics*, Vol. 6, (Am. Cer. Soc., Columbus, OH, 1983).
3. J. Bernasconi, H.P. Klein, B. Knecht, and S. Strassler, *J. Electron. Mater.*, **5**, 473 (1976).
4. R. Einzinger, *Appl. Surf. Sci.*, **1**, 329 (1978).
5. M. Tao, B. Ai, O. Dorlanne, and A. Loubiere, *J. Appl. Phys.*, **61**(4), 1562 (1987).
6. R. Einzinger, *Appl. Surf. Sci.*, **3**, 390 (1979).
7. G.D. Mahan, L.M. Levinson, and H.R. Philipp, *Appl. Phys. Lett.*, **33**, 830 (1978).
8. H.T. Sun, L.Y. Zhang, and X. Yao, *J. Am. Ceram. Soc.*, **76**(5), 1150 (1993).
9. J.T.C. van Kemenade and R.K. Eijnthoven, *J. Appl. Phys.*, **50**(2), 938 (1979).
10. J.D. Russell, D.C. Halls, and C. Leach, *J. Mater. Sci. Lett.*, **14**(9), 676 (1995).
11. E. Olsson and G.L. Dunlop, *J. Appl. Phys.*, **66**(8), 3666 (1989).
12. H. Wang, W. Li, and J.F. Cordaro, *Jpn. J. Appl. Phys.*, **34**(1-4A), 1765 (1995).
13. N. Wakiya, H. Sumino, K. Shinozaki, and N. Mizutani, *J. Ceram. Soc. Jpn.*, **99**(9), 788 (1991).
14. Y.-M. Chiang, W.D. Kingery, and L.M. Levinson, *J. Appl. Phys.*, **53**, 1765 (1982).
15. J. Fleig and J. Maier, *Solid State Ionics*, **85**, 9 (1996).
16. L.F. Lou, *J. Appl. Phys.*, **50**(1), 555 (1979).
17. U. Schwing and B. Hoffmann, *J. Appl. Phys.*, **57**(12), 5372 (1985).
18. M. Matsuoka, *Jpn. J. Appl. Phys.*, **10**(6), 736 (1971).
19. K. Eda, *J. Appl. Phys.*, **49**(5), 2964 (1978).
20. L.M. Levinson and H.R. Philipp, *J. Appl. Phys.*, **46**, 1332 (1975).
21. L.M. Levinson and H.R. Philipp, *J. Appl. Phys.*, **46**, 3206 (1975).
22. L.M. Levinson and H.R. Philipp, *J. Solid State Chem.*, **12**, 292 (1975).
23. K. Eda, *IEEE Electrical Insulation Mag.*, **5**(6), 28 (1989).
24. T.K. Gupta, W.G. Carlson, and P.L. Hower, *J. Appl. Phys.*, **52**, 4104 (1981).
25. M. Hayashi, M. Haba, S. Hirano, M. Okamoto, and M. Watanabe, *J. Appl. Phys.*, **53**, 5754 (1982).
26. J. Fan and R. Freer, *J. Mater. Sci.*, **28**(5), 1391 (1993).
27. N.H. Tri, B. Al, and A. Loubiere, *J. Phys. D: Appl. Phys*, **28**(8), 1723 (1995).
28. S.N. Bai and T.Y. Tseng, *J. Am. Ceram. Soc.*, **78**(10), 2685 (1995).
29. H.F. Li, Y.C. Xu, S.L. Wang, and L.Q. Wang, *J. Mater. Sci.*, **30**(20), 5161 (1995).
30. E.R. Leite, J.A. Varela, and E. Longo, *J. Appl. Phys.*, **72**(1), 147 (1992).
31. A. Bui, K. Alabdullah, A. Loubiere, M. Tao, and Q.C. Nguyen, *J. Phys. D: Appl. Phys.*, **24**(5), 757 (1991).
32. R. Einzinger, *Ann. Rev. Mater. Sci.*, **17**, 299 (1987).
33. K. Eda, A. Iga, and M. Matsuoka, *J. Appl. Phys.*, **51**, 2678 (1980).
34. H.R. Philipp and L.M. Levinson, in *Advances in Electronic Ceramics*, Vol. 7, edited by M.F. Yan and A.H. Heuer (Am. Ceram. Soc., Columbus, OH, 1983), p. 1.
35. T.K. Gupta, W.G. Carlson, and P.L. Hower, *J. Appl. Phys.*, **52**, 4104 (1981).
36. M. Hayashi, M. Haba, S. Hirano, M. Okamoto, and M. Watanabe, *J. Appl. Phys.*, **53**, 5754 (1982).
37. F. Stucki, P. Bruesch, and F. Greuter, *Surface Sci.*, **189/190**, 294 (1987).
38. K. Sato, Y. Tanaka, T. Takemura, and M. Otatake, *J. Appl. Phys.*, **53**, 8819 (1982).